Kirkland and Kamakaka, http://www.jcb.org/cgi/content/full/jcb.201211105/DC1

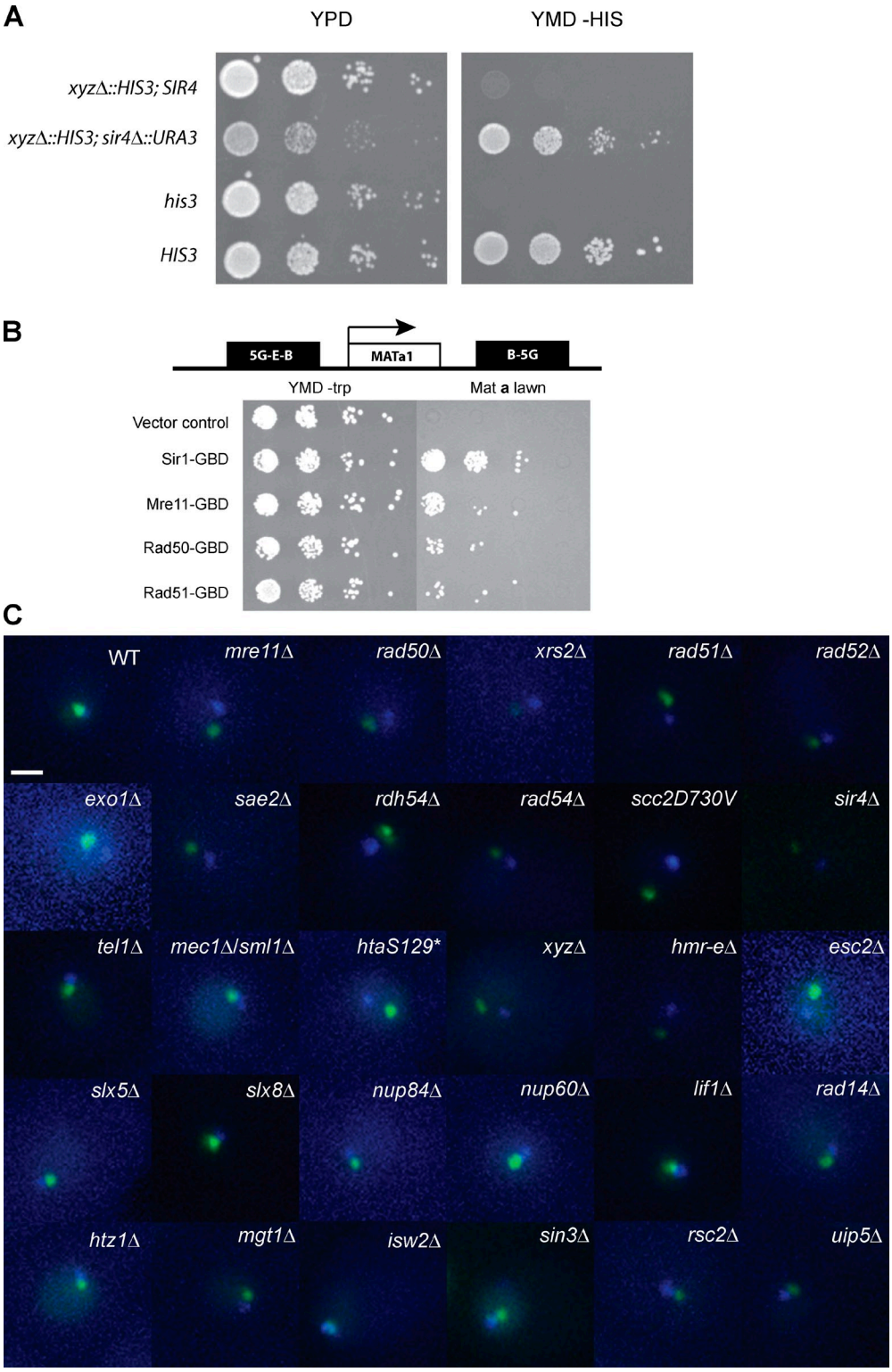

Figure S1. **Silencing controls and representative two-dot assay images.** (A) Silencing in the xyzΔ strain is maintained. Serial dilutions of strains spotted onto YPD growth control (top) or YMD plates lacking histidine (bottom) to assay for silencing of the HIS3 gene inserted in place of the *XYZ* sequence in the heterochromatic region of *HMR*. A strain containing *HIS3* at the *XYZ* locus in a *sir4Δ* background is used as a control for lack of silencing of HIS3. Strains containing the *HIS3* gene or containing a his3-1 mutation at the native *HIS3* locus are used as additional controls. (B) DSB repair proteins and tethered silencing Schematic of constructs containing *5G-E-B* at *HMR-E* and *B-5G* at *HMR-I* flanking the *MATa1* gene. 10-fold serial dilutions on YMD-Trp (growth control) and an a strain lawn (silencing) in an otherwise α strain WT background. Growth signifies silencing of the otherwise active *MATa1* gene. (C) Representative two-dot images. Representative images from WT and mutants in trans-factor assayed in this study. GBD, Gal4 DNA binding domain. Bar, 1,000 nm.

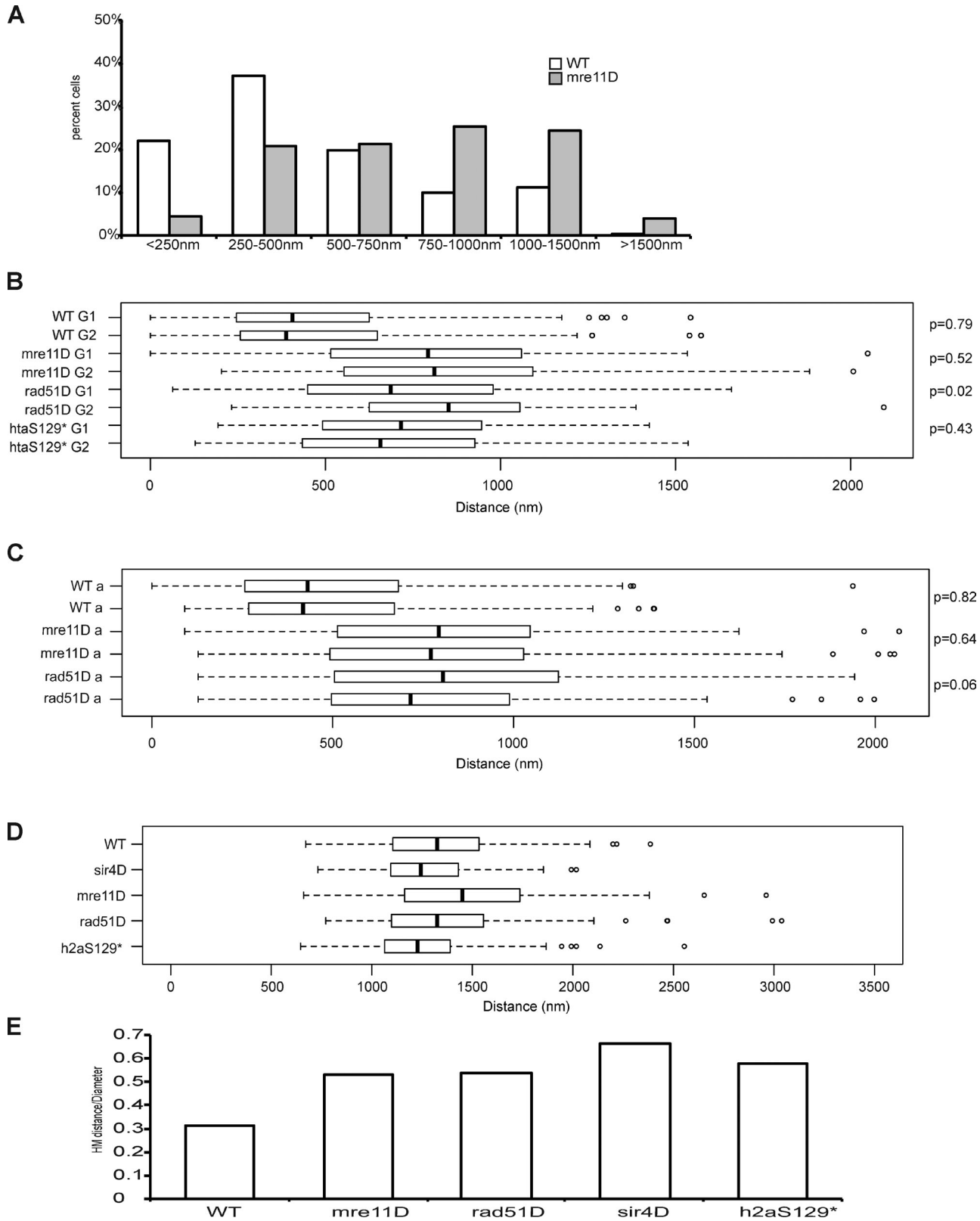

Figure S2. **Controls for HM proximity measurements.** (A) Bar graphs of WT and *mre11Δ* strains (from Fig. 4 A), in which the distance between *HML* and *HMR* are binned into categories of specific distances from two independent strains and three independent trials. Data from each trial was pooled and binned as previously described (Miele et al., 2009); therefore, error bars are not included. (B) Boxplots of the distance between TetR-YFP and CFP-LacI foci in cells of a given strain scored by bud index. Unbudded cells were considered in G1, and budded cells were considered in S/G2. (WT G1, *n* = 192; WT G2, *n* = 136; *mre11Δ* G1, *n* = 103; *mre11Δ* G2, *n* = 93; *rad51Δ* G1, *n* = 157; *rad51Δ* G2, *n* = 105; *htaS129** G1, *n* = 148; and *htaS129** G2, *n* = 106). P-values were calculated using a Mann-Whitney U test (Wilcoxon test) in R. (WT data are the same as presented in Fig. 1 B and are included here to simplify comparison). Data are combined from at least two independent trials. (C) Boxplots of the distance between TetR-YFP and CFP-LacI foci in cells of a given strain in either *MATa* or *MATα* cells. (WTa, *n* = 153; WTα, *n* = 152; *mre11Δ*a, *n* = 221; *mre11Δ*α, *n* = 222; *rad51Δ*a, *n* = 282; and *mre11Δ*α, *n* = 289). P-values were calculated using a Mann-Whitney U test (Wilcoxon test) in R. (D) Boxplots of the distribution of diameters in a given strain. Data presented in B–D are measurements from at least two independent trials. (E) Bar graph of the (median distance of *HM* [from Fig. 4])/(median diameter [from D]) of a given strain. Error bars are not given, as data are simply a ratio of two median measurements. The boxes represent the middle 50% of data points with the black lines showing the median of distances. Outliers are defined as distances >1.5 times the interquartile range (dashed lines) and are represented by open circles.

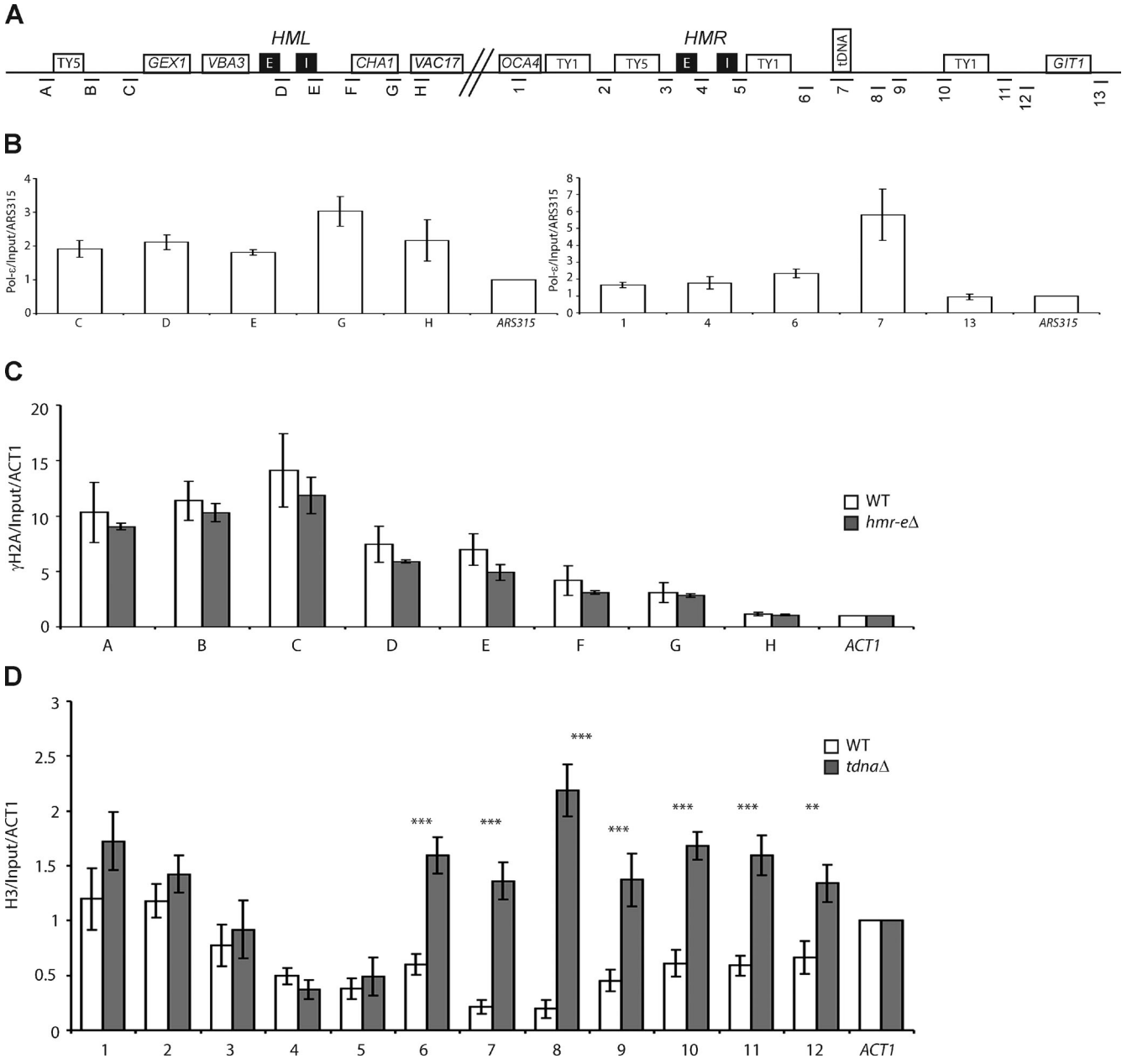

Figure S3. **ChIP at *HM* loci.** (A) Schematic of qPCR amplicons at *HMR* and *HML*. (B) ChIP-qPCR plots of Pol-ε enrichment normalized to *ARS315* at *HMR* and *HML*. Plots are a mean of at least two independent cross-links and four IPs. Error bars are standard deviation from the mean. (C) ChIP-qPCR plots of γH2A enrichment at the *HML* locus in an *hmr-eΔ* strain. (D) ChIP-qPCR plots of H3 enrichment at the *HMR* locus in an *tT(AUG)CΔ* strain. Plots are a mean of three cross-links and six IPs. All amplicons normalized to the *ACT1* locus. WT data are the same as in Fig. 6 and are included for ease of comparison. Error bars are standard deviation from the mean. P-values by *t* test are assigned as ***, P < 0.001; **, P < 0.01; and *, P < 0.05.

Table S1. **Yeast strains used in this study**

ROY No.	Genotype	Experiment
ROY1685	*MATα HMR(s288c) ADE2 his3 leu2 lys2 trp1*	ChIP
ROY1681	*MATα HMR(s288c) ADE2 tT(AGU)CΔ his3 leu2 lys2 trp1 ura3*	ChIP
ROY4819/20	*MATα HMR(s288c) eΔ::URA3 ADE his3 leu2 lys2 trp1*	ChIP
ROY4821/22	*MATa HMR(s288c) Pol-ε-HA::LEU2 lys2 ADE2 his3 lys2 trp1 ura3*	ChIP
ROY4825	*MATa HMR(s288c) SCC2-13×myc::KanMx ADE2 his3 leu2 lys2 trp1 ura3*	ChIP
ROY4826	*MATα HMR(s288c) SCC2-13×myc::KanMx ADE2 hta1S129* hta2S129* his3 leu2 lys2 trp1 ura3*	ChIP
ROY4923/24	*MATα HMR(s288c) SMC6-TAP::HIS3 HMR::S288c ADE2 lys2*	ChIP
ROY4925/26	*MATa HMR(s288c) Mcd1-13×myc::KanMx ADE2*	ChIP
ROY4927/28	*MATα HMR(s288c) BRN1-HA::KanMx ADE*	ChIP
BYS48/ ROY4830	*MATa/α HML-tetO::LEU2 HMR-LacO::TRP1 CFP-LacI tetR-YFP::ADE2 LYS2*	Two-dot microscopy; Miele et al., 2009
ROY4831/32	*MATα/a HML-tetO::LEU2 HMR-LacO::TRP1 CFP-LacI tetR-YFP::ADE2 mre11Δ::HIS3 LYS*	Two-dot microscopy
ROY4833/34	*MATa HML-tetO::LEU2 HMR-LacO::TRP1 CFP-LacI tetR-YFP::ADE2 eΔ::URA3 LYS2*	Two-dot microscopy
ROY4835/36	*MATa HML-tetO::LEU2 HMR-LacO::TRP1 CFP-LacI tetR-YFP::ADE2 xyzΔ::HIS3*	Two-dot microscopy
ROY4837	*MATα HML-tetO::LEU2 leu2-1::LacO(63×)::LEU2 hmrΔ::URA3 CFP-LacI tetR-YFP::ADE2*	Two-dot microscopy
ROY4838	*MATa HML-tetO::LEU2 leu2-1::LacO(63×)::HMR::LEU2 hmrΔ::URA3 CFP-LacI tetR-YFP::ADE2*	Two-dot microscopy
ROY4839/40	*MATa HML-tetO::LEU2 leu2-1::LacO(63×)-HMR::LEU2 hmrΔ::URA3 CFP-LacI tetR-YFP::ADE2 sir4Δ::KanMx*	Two-dot microscopy
ROY4841	*MATa HML-tetO::LEU2 CFP-LacI tetR-YFP::ADE2 LacO(63×)::ChrVI-R::LEU2 hmrΔ::URA3 LYS2*	Two-dot microscopy
ROY4842	*MATα HML-tetO::LEU2 CFP-LacI tetR-YFP::ADE2 LacO(63×)::ChrVI-I::LEU2 hmrΔ::URA3 LYS2*	Two-dot microscopy
ROY4843	*MATα HML-tetO::LEU2 CFP-LacI tetR-YFP::ADE2 LacO(63×)::ChrVI-R::HMR::LEU2 hmrΔ::URA3 LYS2*	Two-dot microscopy
ROY4844	*MATα HML-tetO::LEU2 CFP-LacI tetR-YFP::ADE2 LacO(63×)::ChrVI-I::HMR::LEU2 hmrΔ::URA3 LYS2*	Two-dot microscopy
ROY4929/30	*MATa/α LacO(63×)::ChrVI-16kb::LEU2 LacO963x)::ChrVI-207kb::LEU2 hmrD::URA3 LacI-GFP::ADE2*	Two-dot microscopy
ROY4931/32	*MATa/α LacO(63×)::ChrVI-16kb::HML::LEU2 LacO(63×)::ChrVI-207kb::HMR::LEU2 hmrD::URA3 LacI-GFP::ADE2s*	Two-dot microscopy
ROY4849/50	*MATα/a HML-tetO::LEU2 HMR-LacO::TRP1 CFP-LacI tetR-YFP::ADE2 scc2-D730V::HYG*	Two-dot microscopy
ROY4851/52	*MATa/α HML-tetO::LEU2 HMR-LacO::TRP1 CFP-LacI tetR-YFP::ADE2 rad14Δ::LEU2*	Two-dot microscopy
ROY4853/54	*MATa HML-tetO::LEU2 HMR-LacO::TRP1 CFP-LacI tetR-YFP::ADE2 LYS2 lif1Δ::KanMX*	Two-dot microscopy
ROY4855/56	*MATa/α HML-tetO::LEU2 HMR-LacO::TRP1 CFP-LacI tetR-YFP::ADE2 rad51Δ::HIS3 LYS*	Two-dot microscopy
ROY4859/60	*MAT HML-tetO::LEU2 HMR-LacO::TRP1 CFP-LacI tetR-YFP::ADE2 sir4Δ::URA3 lys-*	Two-dot microscopy
ROY4861/62	*MATa HML-tetO::LEU2 HMR-LacO::TRP1 CFP-LacI tetR-YFP::ADE2 LYS2 exo1Δ::KanMX*	Two-dot microscopy
ROY4863	*MATa HML-tetO::LEU2 HMR-LacO::TRP1 CFP-LacI tetR-YFP::ADE2 rad50Δ::TRP1 LYS*	Two-dot microscopy
ROY4864	*MATa HML-tetO::LEU2 HMR-LacO::TRP1 CFP-LacI tetR-YFP::ADE2 LYS2 sae2Δ::KanMX*	Two-dot microscopy
ROY4865	*MATa HML-tetO::LEU2 HMR-LacO::TRP1 CFP-LacI tetR-YFP::ADE2 xrs2Δ::LEU2 LYS*	Two-dot microscopy
ROY4866/67	*MATa HML-tetO::LEU2 HMR-LacO::TRP1 CFP-LacI tetR-YFP::ADE2 rdh54Δ::KanMX LYS*	Two-dot microscopy
ROY4868/69	*MATa HML-tetO::LEU2 HMR-LacO::TRP1 CFP-LacI tetR-YFP::ADE2 rad54Δ::KanMX LYS*	Two-dot microscopy
ROY4870/71	*Matα/a HML-tetO::LEU2 HMR-LacO::TRP1 CFP-LacI tetR-YFP::ADE2 esc2Δ::HIS3 lys2*	Two-dot microscopy
ROY4872/73	*MATa HML-tetO::LEU2 HMR-LacO::TRP1 CFP-LacI tetR-YFP::ADE2 rad52Δ::KanMX LYS*	Two-dot microscopy
ROY4876/77	*MATa HML-tetO::LEU2 HMR-LacO::TRP1 CFP-LacI tetR-YFP::ADE2 LYS2 tel1Δ::KanMX*	Two-dot microscopy
ROY4878/79	*MATα HML-tetO::LEU2 HMR-LacO::TRP1 CFP-LacI tetR-YFP::ADE2 mec1Δ::HIS3 sml1Δ::KanMX*	Two-dot microscopy
ROY4880/81	*MATα/a HML-tetO::LEU2 HMR-LacO::TRP1 CFP-LacI tetR-YFP::ADE2 LYS hta1S129* hta2S129**	Two-dot microscopy
ROY4882/83	*MATa HML-tetO::LEU2 HMR-LacO::TRP1 CFP-LacI tetR-YFP::ADE2 nup60Δ::KanMX LYS*	Two-dot microscopy
ROY4884/85	*MATa HML-tetO::LEU2 HMR-LacO::TRP1 CFP-LacI tetR-YFP::ADE2 LYS2 slx5Δ::KanMX*	Two-dot microscopy
ROY4886/87	*MATa/α HML-tetO::LEU2 HMR-LacO::TRP1 CFP-LacI tetR-YFP::ADE2 LYS2 nup84Δ::KanMX*	Two-dot microscopy
ROY4888/89	*MATa HML-tetO::LEU2 HMR-LacO::TRP1 CFP-LacI tetR-YFP::ADE2 LYS2 slx8Δ::KanMX*	Two-dot microscopy
ROY4894/95	*MATa YIPLac-HDEL-dsRED::NatMx HMR-GIT1-LacO(256×)::TRP LacI-GFP::ADE2 RECR::LEU2 ura3 his3 rad51Δ::KanMx*	Zone analysis
ROY4896/97	*MATa YIPLac-HDEL-dsRED::NatMx HMR-GIT1-LacO(256×)::TRP LacI-GFP::ADE2 RECR::LEU2 ura3 his3 mre11Δ::KanMx*	Zone analysis
ROY4898/99	*MATa/α HML-tetO::LEU2 HMR-LacO::TRP1 CFP-LacI tetR-YFP::ADE2 LYS2 rsc2Δ::KanMX*	Two-dot microscopy
ROY4900/01	*MATa/α HML-tetO::LEU2 HMR-LacO::TRP1 CFP-LacI tetR-YFP::ADE2 isw2Δ::KanMx LYS*	Two-dot microscopy
ROY4902/03	*MATa HML-tetO::LEU2 HMR-LacO::TRP1 CFP-LacI tetR-YFP::ADE2 mgmt1Δ::KanMX LYS*	Two-dot microscopy
ROY4904/05	*MATa HML-tetO::LEU2 HMR-LacO::TRP1 CFP-LacI tetR-YFP::ADE2 uip5Δ::KanMX LYS*	Two-dot microscopy
ROY4906/07	*MATα/a HML-tetO::LEU2 HMR-LacO::TRP1 CFP-LacI tetR-YFP::ADE2 sin3Δ::KanMx*	Two-dot microscopy
ROY4908/09	*MATα/a HML-tetO::LEU2 HMR-LacO::TRP1 CFP-LacI tetR-YFP::ADE2 htz1Δ::KanMx LYS*	Two-dot microscopy
ROY4942/43	*MATα/a HML-tetO::LEU2 HMR-LacO::TRP1 CFP-LacI tetR-YFP::ADE2 smc6-9::NatMx LYS*	Two-dot microscopy
ROY4944	*MATα 5GEB-a1-B5G::HMR LYS*	Silencing

All strains are isogenic to W303 except when noted with an asterisk.

Table S2. **qPCR primers used in this study**

Name	Sequence 5′ → 3′	Amplicon
GRO40	ATTTATTAATGTCAAAAGCCGCTGAGG	1
GRO39	TAAGACAATTGTGGACAACAAAGCAAA	1
GRO51	AAAACAACGCGTCATGAAAAAGAGTTA	2
GRO52	ATCACGTTCAACAAGGAACTCTACCAA	2
GRO49	TTATAAAATCCTCGCACTATCGCTGTT	3
GRO50	TGGGTTAGAGATTTGCAACTATTTTCTTC	3
LOU191	CCCGTCCAAGTTATGAGCTTAATC	4
L95	AAAACCAGGAGTACCTGCGCTTATTCT	4
L97	TAATACCTTTAAATGTTGAGGTAAATAGC	5
L98	GCTAAAGTGTGTGGAAAAACATTTTCTTGT	5
Lou201	CACCAATTCCGCATCTGCAGATTAC	6
L96	GGTAGAATGACCTAGAATGACCCATC	6
R197	GAGACCAGGTTTATTCAACCGGTAAC	7
Lou120	GGGTGTCACCGAATAACGTGAT	7
R189	ATCACGTTATTCGGTGACACCCAG	8
R190	GCCGTAAGAGATCTCCGAATAACGGTA	8
L108	TACCGTTATTCGGAGATCTCTTACGG	9
L109	GTGACGCACTGAATGTCATCAAAAG	9
R191	CTTTTGATGACATTCAGTGCGTCAC	10
R192	ACCGGATATAGAAGAACTCGTCTTATG	10
L104	CATAAGACGAGTTCTTCTATATCCGGT	11
L107	CCTATTTTGCGTATTCCTATGTTG	11
R193	CTAAGACGCTAGGACTTCTAAACACAGA	12
R194	ACCATATTGCTTAATTTCTTACTACTTG	12
GRO61	GAGTGTCCGCATGATTAATACTTTTCG	13
GRO62	ATATGAAGATAAATGTGGCACCAAACG	13
QJK33	TTGCAAATTGCTTGAACGGATGCCATT	A
QJK34	TACCGGATTAGAGGTTTGCTACTATATG	A
QJK45	AATTCACTACGTCAACATATCCCACG	B
QJK46	GAGGCCGTAGGGACATATAGCA	B
QJK35	GGCTGTACCATGTAAAATGAGCGG	C
QJK36	CCTTTTGAGATTCTTCACCAATGTTGC	C
R225	GTACTTAGTATTTGGCCATTATTATCG	D
R226	TTACATTTCATTCTATGTGCGCTAGAT	D
R227	AGCTGAGTAACTAACTCTCATGGTACA	E
R228	GAAGTAAGTTAACATAGAAGTCAAACAC	E
QJK47	CTGCAGCATGTCCCCCTTTATACA	F
QJK48	GTGTAAGATTTCTCGAAGTAAGCATCAA	F
QJK51	CAAAACCGGCATTACCGCCAGAA	G
QJK52	AACCAAGTGGCTCCTTCAAAAGTAGA	G
QJK49	TCTGTTCGAGACAAGTTGAGCAAGG	H
QJK50	CCAGCTCGTTCAACCTCAAAGTGA	H
JK250	CTTTCTCCACCACTGCTGAAAGAG	ACT1
JK252	GAAGAAGATTGAGCAGCGGTTTGC	ACT1
R219	GTTACGACGAAGCACGGCAAATTAG	ARS315
R220	AAAACGGTCCGCTAAGAGCCGGTA	ARS315

Reference

Miele, A., K. Bystricky, and J. Dekker. 2009. Yeast silent mating type loci form heterochromatic clusters through silencer protein-dependent long-range interactions. *PLoS Genet.* 5:e1000478. http://dx.doi.org/10.1371/journal.pgen.1000478